Effects of Ga doping in $La_{2/3}Sr_{1/3}MnO_3$

Javier Blasco,* Joaquín García, and Jolanta Stankiewicz
Instituto de Ciencia de Materiales de Aragón and Departamento de Física de la Materia Condensada, Consejo Superior de Investigaciones Científicas y Universidad de Zaragoza, 50009 Zaragoza, Spain

(Received 24 February 2003; revised manuscript received 19 May 2003; published 26 August 2003)

We substitute Ga for Mn in the $La_{2/3}Sr_{1/3}MnO_3$ compound to see how magnetic and atomic disorder affects the properties of this system. Ga doping gives rise to minor structural effects in the $La_{2/3}Sr_{1/3}Mn_{1-x}Ga_xO_3$ ($0 \leqslant x \leqslant 0.5$) series. However, the Curie temperature and the temperature at which the resistivity changes its behavior from insulating- to metallic-like both decrease drastically with increasing Ga content. In addition, these transitions do not occur at the same temperature for $x > 0.02$. Ferromagnetic long-range order is observed for samples with $x < 0.3$. For $x > 0.3$, the system is in a spin-glass-like state. We obtain rather high values of negative magnetoresistance in $x \leqslant 0.2$ samples, which likely arises from spin-polarized tunneling.

DOI: 10.1103/PhysRevB.68.054421 PACS number(s): 75.47.De, 71.30.+h, 75.10.Nr, 61.10.−i

I. INTRODUCTION

Physical properties of manganites (mixed oxides of Mn and rare earths R), in particular the colossal magnetoresistance, have attracted a lot of attention in recent years.[1] The introduction of a divalent cation A (A=Ca, Sr, Ba) onto the trivalent R site gives rise to a mixed valence of Mn atoms. Above some critical value of x, $R_{1-x}A_xMnO_3$ undergoes a paramagnetic (PM) to ferromagnetic (FM) transition coupled with a sharp decrease in resistivity upon cooling.[2] The highest transition temperature (T_C) is observed for $x \sim 1/3$.[1,2] The double exchange interaction is considered the main mechanism controlling both the magnetic and transport properties in manganites.[3] However, there are some puzzling phenomena in their behavior, which are not well understood. Additional mechanisms such as electron-phonon coupling,[4] the average ionic size of cations (R, A),[5,6] the size mismatch[7] between R and A cations or atomic disorder contribute to the physical properties of this system. In order to account for the role of disorder in the Mn sublattice, several groups have studied the effect of substitution of Mn ions with other elements. Some have used magnetic elements (such as Fe or Cr) in their studies.[8–12] However, in this case it is difficult to separate new magnetic interactions from disorder effects. Other have used nonmagnetic elements but with a large size-mismatch that could induce microscopical strain and lattice distortions.[13,14] Among several alternatives, the introduction of the nonmagnetic Ga^{3+} onto the Mn sites seems to be the best way to minimize lattice strain since Mn^{3+} and Ga^{3+} have similar ionic sizes.[15] Such a substitution has been studied earlier in the $La_{2/3}Ca_{1/3}Mn_{1-x}Ga_xO_3$ system, where a sharp decrease of T_C with the increasing content of Ga has been found.[16,17] The FM long-range order disappears between $x=0.1$ and 0.25 in this system. Only a few studies have been devoted to the investigation of Ga doping in the $La_{2/3}Sr_{1/3}MnO_3$ compound. Some have focused on the study of heavy doped manganites $La_{1-x}Sr_xMn_{1/2}Ga_{1/2}O_3$, looking for the correlation between the Mn^{+4} concentration and changes in structural and magnetic properties.[18,19] Properties of $La_{2/3}Sr_{1/3}Mn_{0.9}M_{0.1}O_3$ (M=Ga, Ni, and Fe) were reported in Ref. 9. The Ga-substituted compound shows a large decrease of the temperature corresponding to both magnetic and resistive (from semiconducting to metallicklike behavior) transitions. On the other hand, effects of disorder on the properties of manganites have been calculated by several groups.[20–22] They found that the Curie temperature decreases with increasing disorder. An uncoupling of magnetic and resistive transitions for sufficiently high degrees of disorder has been also foreseen.[20,22] With the aim of verifying this prediction and to gain some insight into the behavior of the $La_{2/3}Sr_{1/3}Mn_{1-x}Ga_xO_3$ system, we have performed a careful study of this series for $x \leqslant 0.5$. We have measured magnetic and electrical transport properties in a broad range of temperature and magnetic field. Our results show that, indeed, the magnetic and resistive transitions are uncoupled in the $0.05 \leqslant x \leqslant 0.2$ range.

II. EXPERIMENT

The samples of $La_{2/3}Sr_{1/3}Mn_{1-x}Ga_xO_3$ (x=0, 0.02, 0.05, 0.08, 0.1, 0.15, 0.2, 0.3, 0.4, and 0.5) were prepared by a solid state reaction. Stoichiometric amounts of La_2O_3, $SrCO_3$, $MnCO_3$, and Ga_2O_3 with a nominal purity of not less than 99.95% were mixed and heated in air at 950 °C for 18 h. After grinding, they were pressed into bars and sintered in air at 1250 °C for 18 h and at 1500 °C for 48 h with intermediate grindings. The oxygen content was analyzed by iodometric titration. All samples were stoichiometric within the experimental error (oxygen content of 3 ± 0.015).

Step-scanned powder diffraction patterns were collected between 19° and 140° (in steps of 0.03°) at room temperature using a D-max Rigaku system with a Cu rotating anode. The device was working at 40 kV and 80 mA with a counting rate of 4 sec step^{-1}. A graphite monochromator was used to select the Cu K_α radiation. The crystal structures were refined by the Rietveld method using the FULLPROF program.[23]

Magnetic measurements were performed between 5 and 380 K and up to 5 T in a commercial Quantum Design superconducting quantum interference device magnetometer provided with an ac experimental setup. Resistivity measurements on the same samples were carried out using the standard six-probe ac method in the temperature range from 4 to 500 K and in magnetic fields of up to 5 T.

TABLE I. Structural parameters (lattice parameters, volume, fractional atomic coordinate and isotropic displacement factors) and some reliability factors (defined as in Ref. 23) for $La_{2/3}Sr_{1/3}Mn_{1-x}Ga_xO_3$ ($x \leqslant 0.5$) at 300 K. Digits in parentheses refer to standard deviations.

Sample	$x=0$	$x=0.02$	$x=0.05$	$x=0.08$	$x=0.1$	$x=0.15$	$x=0.2$	$x=0.3$	$x=0.4$	$x=0.5$
a (Å)	5.5001(1)	5.4995(1)	5.4994(1)	5.4991(1)	5.4978(1)	5.4967(1)	5.4945(2)	5.4912(1)	5.4866(1)	5.4837(1)
c (Å)	13.3593(2)	13.3568(2)	13.3517(3)	13.3474(2)	13.3469(2)	13.3427(2)	13.3417(2)	13.3362(2)	13.3288(2)	13.3237(1)
Volume (Å^3)	349.99(1)	349.84(1)	349.70(1)	349.55(1)	349.37(1)	349.13(1)	348.85(2)	348.26(1)	347.49(1)	346.98(1)
La at (0 01/4):										
B (Å^2)	0.49(1)	0.26(1)	0.31(2)	0.66(1)	0.35(1)	0.35(1)	0.35(1)	0.46(1)	0.38(1)	0.47(1)
Mn/Ga (0 00):										
B (Å^2)	0.25(1)	0.10(2)	0.15(2)	0.45(1)	0.16(2)	0.12(2)	0.19(2)	0.22(2)	0.18(2)	0.32(1)
O (x 01/4):										
x	0.5408(6)	0.5406(7)	0.5404(9)	0.5402(6)	0.5401(7)	0.5401(8)	0.5399(7)	0.5400(7)	0.5400(7)	0.5394(7)
B (Å^2)	1.18(7)	0.63(7)	0.99(9)	1.02(7)	0.66(7)	0.98(8)	0.56(7)	0.89(7)	1.09(8)	0.69(7)
$R_{wp}(\%)/R_{Bragg}(\%)$	8.6/3.9	11.4/5.2	11.6/4.2	9.3/4.0	10.2/4.1	11.3/4.3	9.9/4.0	9.9/4.3	10.2/4.8	9.9/3.8

III. RESULTS

A. Structure at room temperature

X-ray powder diffraction studies revealed that a unique phase could be formed over the range of x between 0 and 0.5 in the $La_{2/3}Sr_{1/3}Mn_{1-x}Ga_xO_3$ system. Only the $x=0.5$ sample showed an impurity (around 1% of $LaSrGa_3O_7$) that was included in the refinement as a secondary phase.[24] The diffraction patterns obtained can be successfully refined for all samples in the frame of the $R\bar{3}c$ space group, very common for slightly distorted perovskites (it corresponds to an $a^-a^-a^-$ octahedral tilt scheme with equal rotations about all three pseudocubic axes[25]). A monoclinic cell, the $I2/c$ space group, has been claimed for $x=0.5$ on the basis of an electron diffraction study.[19] Since the additional distortion corresponding to this structure is very small (undistinguishable by x-ray diffraction) and both space groups give accurate Rietveld fittings, we have also analyzed the $x=0.5$ sample in the rhombohedral group. Structural parameters obtained from Rietveld analysis are summarized in Table I.

The volume of the refined unit cell decreases as the content of Ga increases in $La_{2/3}Sr_{1/3}Mn_{1-x}Ga_xO_3$. This decrease is almost linear with x, and amounts up to approximately -6.2 Å^3 per Ga atom. The variation of the lattice parameters with x is more complex. The rate at which the lattice constant, corresponding to the c axis, decreases with x is almost uniform. However, the rate for the a axis varies strongly with composition: it is small for $x<0.1$ and large for $x \geqslant 0.1$. The inflection point coincides with the conductivity character change in the $La_{2/3}Sr_{1/3}Mn_{1-x}Ga_xO_3$ system which, at room temperature, is metallic up to $x \sim 0.08$ (see below). Figure 1 shows the refined M-O distances (M=Mn, Ga) and the M-O-M bond angles as a function of the Ga content. The M-O length decreases with increasing x as expected for the substitution of Mn^{3+} by Ga^{3+}. It varies between 1.952 ($x=0$) and 1.945 Å ($x=0.5$). We note that the M-O distance found for the undoped compound is slightly below the calculated one from the tabulated ionic radii (1.956 Å). The Mn^{3+} ion in high spin state usually shows Jahn-Teller distortion that is absent in metallic manganites.[26] Therefore, the addition of the tabulated ionic radii must only be considered as a rough approximation in the present case. The M-O distances, shown in Fig. 1, decrease almost linearly with x in the $La_{2/3}Sr_{1/3}Mn_{1-x}Ga_xO_3$ series with a rate of -0.012 Å per Ga atom. This finding, and bearing in mind the ionic sizes[15] for Mn^{3+}, Mn^{4+}, and Ga^{3+} (0.645, 0.53, and 0.62 Å, respectively), lead us to conclude that Ga^{3+} replaces Mn^{3+} in the manganite lattice. In addition, we found that the oxygen stoichiometry, determined by iodometric titration, is not affected by Ga doping. This leads to an increase of the Mn^{4+}/Mn^{3+} ratio as the content of Ga does.

Finally, the M-O-M bond-angle slightly increases as the Ga content increases, varying between 166.8° for $x=0$ and 167.25° for $x=0.5$. This curve shows a plateaulike behavior for $0.1 \leqslant x \leqslant 0.3$. Nevertheless, the structural changes are very small as expected for the substitution of Mn^{3+} with an ion of a similar ionic size.

B. Magnetic properties

Figure 2 shows the temperature dependence of the in-phase ac susceptibility (χ_{ac}) for $x \leqslant 0.3$ compounds. The x

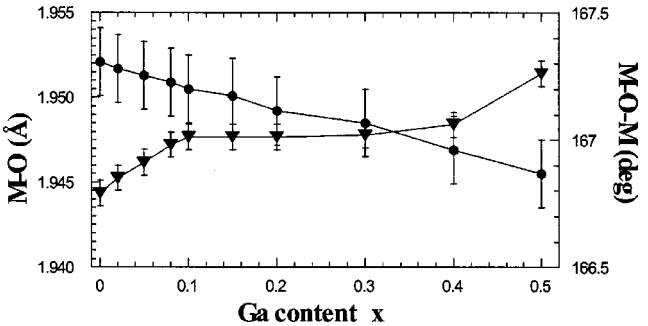

FIG. 1. Interatomic M-O distances (circles) and M-O-M bond angles (triangles) for $La_{2/3}Sr_{1/3}Mn_{1-x}Ga_xO_3$ samples with $x \leqslant 0.5$. M refers to Mn/Ga.

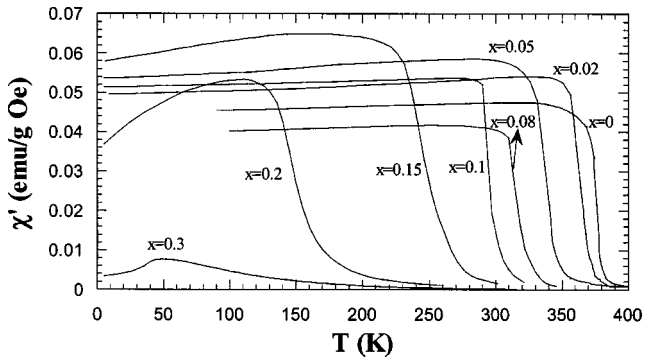

FIG. 2. The in-phase magnetic susceptibility for $La_{2/3}Sr_{1/3}Mn_{1-x}Ga_xO_3$ samples ($x \leqslant 0.3$).

$\leqslant 0.2$ samples clearly show ferromagnetic transitions. The critical temperature T_C, defined as the inflection point of the χ_{ac} curve, decreases as the Ga content increases. T_C varies from 365 to 152 K as x goes from 0 to 0.2, respectively. The χ_{ac} (T) variations, measured at different frequencies of the ac field, are shown in Fig. 3 for $x \geqslant 0.3$ compounds. These curves peak at a low temperature between 49.5 and 15.5 K as x varies from 0.3 to 0.5, respectively. The maximum of $\chi_{ac}(T)$ decreases in amplitude and shifts to higher temperatures as the frequency of the ac field increases. Such a behavior can be attributed to a dynamic spin freezing and, likely, the FM long-range order is not achieved in these samples. In fact, neutron diffraction experiments did not show any FM ordering for the $x=0.5$ sample.[19] None of the samples studied obeys the Curie-Weiss law in the temperature range studied (below 400 K).

Magnetic loops were measured at 5 K for all samples studied. The results are displayed in Fig. 4. All of the $La_{2/3}Sr_{1/3}Mn_{1-x}Ga_xO_3$ samples show a spontaneous magnetization at 5 K. However, the samples with $x \leqslant 0.2$ behave as soft ferromagnets. Magnetic saturation is already achieved at magnetic fields of approximately 5 kOe. The obtained saturated magnetic moment M_S decreases almost linearly with x in this composition range with a rate of $-4.6\mu_B$/Ga atom [see inset (a)]. M_S varies between $3.87\mu_B$/fu and $2.90\mu_B$/fu as x changes between 0 and 0.2, respectively. The value of the magnetic moment M_S found for the parent compound,

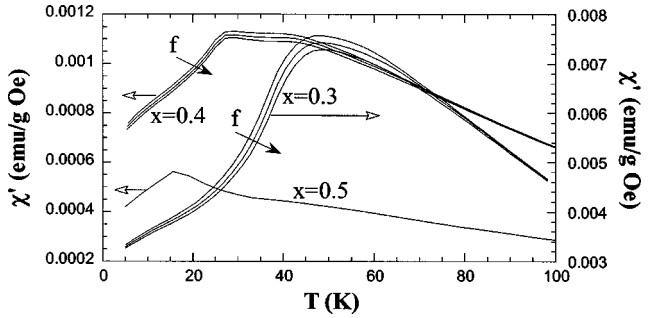

FIG. 3. The in-phase magnetic susceptibility for $La_{2/3}Sr_{1/3}Mn_{1-x}Ga_xO_3$ samples ($0.3 \leqslant x \leqslant 0.5$). Samples with $x=0.3$ and 0.4 were measured at different frequencies of the alternating field (1, 10, and 100 Hz). Arrows indicate the frequency (f) increase.

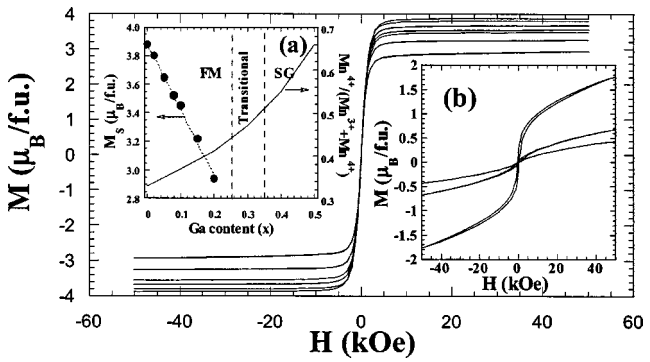

FIG. 4. Magnetization vs field at 5 K for (from top, highest M, to bottom): $x=0$, 0.02, 0.05, 0.08, 0.1, 0.15, and 0.2 samples. Inset (a): Saturated magnetization (points) and $Mn^{4+}/(Mn^{3+}+Mn^{4+})$ ratio (solid line) vs x for $La_{2/3}Sr_{1/3}Mn_{1-x}Ga_xO_3$ samples. The dotted line shows a linear fit while vertical broken lines are posible limits for different magnetic phases. FM and SG denote ferromagnetic and spin-glass regions, respectively. Inset (b): Magnetization vs field at 5 K for (from top, highest M, to bottom) $x=0.3$, 0.4, and 0.5 samples.

$x=0$, is higher than the expected one for the spin-only contribution with $g=2$ ($3.67\mu_B$/fu). The similar finding has been reported earlier.[27] Nevertheless, the agreement between calculated and experimental M_S values ($2.87\mu_B$/fu and $2.90\mu_B$/fu, respectively) is excellent for $x=0.2$.

The magnetic properties of the $x=0.3$ compound are noteworthy. This sample shows a large spontaneous magnetization, but its saturation is not achieved at 5 T [see inset (b)]. The magnetic moment at 5 T is $1.76\mu_B$/fu, far below the expected one for a fully polarized Mn sublattice. Moreover, the magnetization curve has a positive slope at high magnetic fields, indicating the presence of either a canted ferromagnetic arrangement or a secondary paramagnetic phase. An inhomogeneous magnetic state cannot be discarded as well, bearing in mind the dynamic behavior shown by $\chi_{ac}(T)$ in this sample (see Fig. 3). Neutron experiments are desirable to shed some light on this subject.

Samples with a higher Ga content exhibit smaller spontaneous magnetization values. The positive slope of the magnetization curves at high magnetic fields in addition to the low magnetic moment at 5 T is consistent with lack of the long-range FM order in these materials. Both samples ($x=0.4$ and 0.5) are likely in a (spin or cluster-) glass state at low temperatures as proposed recently for $x=0.5$ from neutron diffraction experiments.[19]

The substitution of Mn by Ga changes the Mn^{4+}/Mn^{3+} ratio in $La_{2/3}Sr_{1/3}Mn_{1-x}Ga_xO_3$ samples. This is shown in the inset of Fig. 4, where $Mn^{4+}/(Mn^{4+}+Mn^{3+})$ is plotted versus x. FM ordering is observed for $Mn^{4+}/(Mn^{4+}+Mn^{3+})$ up to approximately 0.47.

C. Current transport properties

How the resistivity ρ of the $La_{2/3}Sr_{1/3}Mn_{1-x}Ga_xO_3$ series varies with temperature is shown in Fig. 5. As the content of Ga increases, the material studied becomes more resistive. We have noted that the repeated annealing of the bars re-

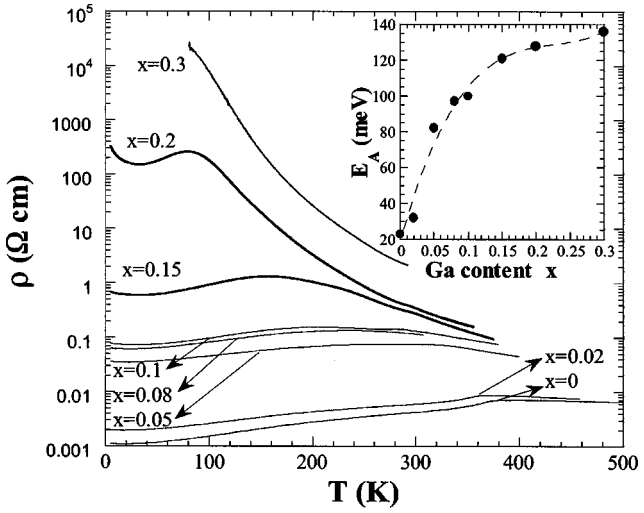

FIG. 5. Resistivity vs temperature for the $La_{2/3}Sr_{1/3}Mn_{1-x}Ga_xO_3$ ($x \leqslant 0.3$) samples. Inset: Variation of the activation energy with the content of Ga ($x \leqslant 0.3$). The broken line is a guide for the eye.

duces their electrical resistance significantly but without changing the shape of the $\rho(T)$ curves as reported earlier for $La_{1-x}Sr_xMnO_3$ samples.[28] Here, we present results for samples prepared at the same conditions (annealing for 48 h at 1500 °C). The $x=0$ compound exhibits a sharp drop of the resistivity below 360 K, close to the T_C, in agreement with the previously reported results for the polycrystalline $La_{2/3}Sr_{1/3}MnO_3$ system.[27,28] For x up to 0.2, $\rho(T)$ shows a maximum which we ascribe to the resistive transition between insulating ($d\rho/dT<0$) and metallic ($d\rho/dT>0$) conductivity regimes. The temperature for this transition, T_M, decreases as the content of Ga increases. The $x=0.3$ composition is semiconducting in the whole range of temperature studied. For $T>T_M$, the resistivity of $x \leqslant 0.3$ samples follows the Arrhenius law: $\rho \propto \exp(E_A/kT)$. We plot the activation energy (E_A) vs composition in the inset of Fig. 5. E_A increases with the increasing content of Ga and tends to saturate at a value of approximately 140 meV for large x. The observed behavior could be attributed to both the diminution of hopping paths when Ga^{3+} replaces Mn^{3+} (the former, with a $3d^{10}$ electronic configuration, does not participate in the electronic conduction) and the change in the Mn^{4+}/Mn^{3+} ratio.

In Fig. 6 we compare the magnetic and resistive behavior for various $La_{2/3}Sr_{1/3}Mn_{1-x}Ga_xO_3$ samples. First, we note that T_C and T_M almost coincide for the low Ga doping ($x \leqslant 0.02$), as expected for coupled transitions [Fig. 6(a)]. However, for the higher doping ($x \geqslant 0.05$) the resistivity has a maximum at temperatures much lower than T_C [Fig. 6(b)]. A similar behavior has also been observed in other substituted manganites.[10,12,17] The difference between T_C and T_M can sometimes arise from the procedure used in defining T_C. Some authors define T_C as the temperature corresponding to the inflection point in the magnetization curve (the criterion used here) whereas others prefer to extrapolate the maximum slope of the magnetization curve to the T axis. However, this is not our case as T_C and T_M differ by more than 30% in some compositions.

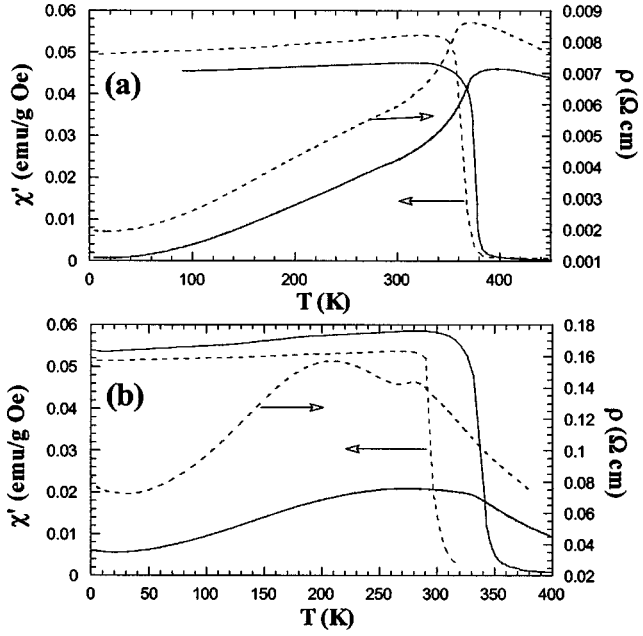

FIG. 6. Comparison between $\rho(T)$ and $\chi'(T)$ curves for $La_{2/3}Sr_{1/3}Mn_{1-x}Ga_xO_3$ samples with (a) $x=0$ (continuous line) and $x=0.02$ (dotted line), and (b) $x=0.05$ (continuous line) and $x=0.1$ (dotted line).

Usually, replacing Mn with other elements in manganites leads to a broadening of the magnetic transition. For high enough doping, the long-range magnetic ordering is lost and the magnetic curve shows a peak typical of cluster or spin-glass systems. The resistive transition (if existing) in such systems is observed either at the magnetic peak or at the low-temperature onset of the magnetic transition. The present case shows significant differences: First, the magnetic transition remains sharp for all the compositions showing the resistive transition which for $0.05 \leqslant x \leqslant .0.2$ takes place well below T_C. In addition, the resistivity exhibits some anomalies at the magnetic transition such as a kink [see the $x=0.05$ curve in Fig. 6(b)] or a clear peak [$x=0.1$ in Fig. 6(b)]. The kink at T_C is hardly visible in the $\rho(T)$ curve for other compositions (such as $x=0.2$, not shown here) but it appears in the first derivative. We note that $x=0.2$ and 0.15 have rather high electrical resistivities in their ''metallic'' phase.

Finally, we find that the resistivity of all $La_{2/3}Sr_{1/3}Mn_{1-x}Ga_xO_3$ samples studied show a minimum at low temperatures. The temperature corresponding to this minimum increases as the Ga content increases. This feature might also be related to the polycrystalline nature of the samples because the minimum in the resistivity is not observed in single crystals of $La_{2/3}Sr_{1/3}MnO_3$.[27] However, the dependence on the content of Ga suggests an intrinsic character.

D. Magnetoresistance

The uncoupling between magnetic and electrical transitions leads to the following question: how are they affected by an external magnetic field? In order to answer this ques-

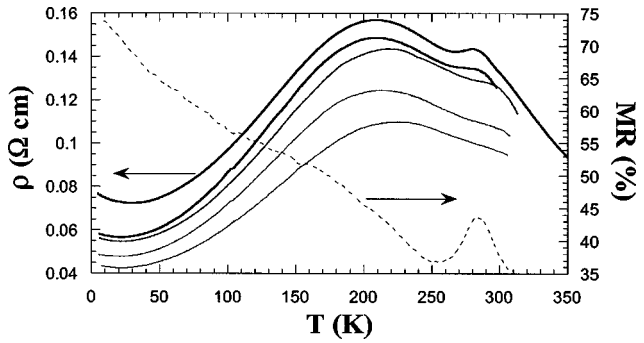

FIG. 7. Resistivity vs temperature at different external magnetic fields (continuous line) and temperature dependence of the magnetoresistance (dotted line) for $La_{2/3}Sr_{1/3}Mn_{0.9}Ga_{0.1}O_3$. The values of the magnetic field are (from top to bottom): 0, 5, 10, 30, and 50 kOe. The magnetoresistance is defined as $MR(\%)=100\times[\rho(H=0,T)-\rho(H=50\ \text{kOe},T)]/\rho(H=50\ \text{kOe},T)$.

tion, we have focused this part of the study on the $x=0.1$ sample, where both transitions are clearly distinguishable. Resistivity variations at different external magnetic fields are shown in Fig. 7. The resistivity decreases as the applied field increases. It is clear that the anomaly associated with the magnetic transition shifts towards higher temperatures with increasing magnetic field. The resistivity maximum, however, remains almost at the same temperature. On the other hand, the shallow minimum at ~ 30 K shifts towards lower temperatures upon applying a magnetic field. The magnetoresistance, defined as $[\rho(H=0,T)-\rho(H=50\ \text{kOe},T)]/\rho(H=50\ \text{kOe},T)$, is also displayed in the same figure. Two contributions to magnetoresistance are clearly seen: One at high temperature (peak shape), arising from the shift of T_C, and another below T_C likely related to the grain boundaries. In Fig. 8 we show $\rho(H)/\rho(0)$ versus H and $[\rho(H)-\rho(50\ \text{kOe})]/\rho(0)$ versus $[M/M(50\ \text{kOe})]^2$ curves for the $x=0.1$ sample in the temperature range from 5 to 300 K ($[\rho(H)-\rho(50\ \text{kOe})]/\rho(0)$ is some measure of the magnetic resistivity). At low fields, the resistivity drops sharply in the ferromagnetic region. This drop is larger at lower temperatures and reaches values close to 25% at 5 K. In the same field range, the magnetization increases sharply. The variation of $[\rho(H)-\rho(50\ \text{kOe})]/\rho(0)$ is almost linear with the square of the normalized magnetization in this region. At higher fields, the resistivity still decreases, though magnetic saturation has been achieved. Thus, two regimes are observed in the variation of the resistivity in the ferromagnetic region. On the other hand, in the paramagnetic region the magnetic resistivity varies almost linearly with $[M/M(50\ \text{kOe})]^2$ in the whole range of fields studied.

IV. DISCUSSION AND CONCLUSIONS

Ga doping in the $La_{2/3}Sr_{1/3}Mn_{1-x}Ga_xO_3$ system gives rise to several effects: (i) an enhancement of the disorder, (ii) a decrease of the conduction paths for electrons as Ga^{3+} ions do not participate in conduction, (iii) a partial suppression of both the ferromagnetic double-exchange and superexchange antiferromagnetic interactions since Ga^{3+} ions do not have a

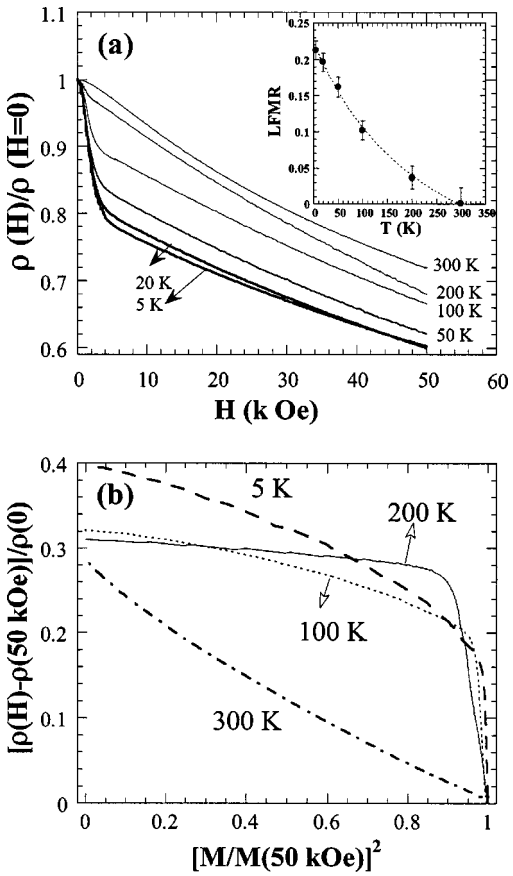

FIG. 8. (a) Field dependence of $\rho(H)/\rho(H=0)$ at the temperatures indicated in the figure for $La_{2/3}Sr_{1/3}Mn_{0.9}Ga_{0.1}O_3$. Inset: Temperature dependence of the low-field magnetoresistance (LFMR) and the best fit (see Ref. 27) of the form $\text{LFMR}\ (T)=a+b/(T+c)$ (dashed line). The fitting parameters are $a=-0.18$, $b=103$ K, and $c=248$ K. (b) Magnetic resistivity, $[\rho(H)-\rho(50\ \text{kOe})]/\rho(0)$, vs $[M/M(50\ \text{kOe})]^2$ at different temperatures for the same sample.

core spin, and (iv) an on-site electrostatic perturbation. The latter is a consequence of the fact that the average valence of the Mn-Ga-Mn sublattice ($+3.3$) is higher than that of Ga^{3+}. Holes cannot hop onto Ga sites, but they stay longer at the Mn ion which neighbors with Ga.[22] The disorder is not only enhanced by the random substitution of Ga atoms for Mn but also by lattice distortions arising from the different ionic sizes of the dopant. All these factors affect the properties of the system studied. We discuss some of them below.

A. Structural properties

The structural changes related to the Ga doping are minor, as expected for the substitution of Mn^{+3} with an ion of a similar ionic size. Only a small decrease of the M-O distance in addition to a slight increase of the M-O-M bond angle, are found. Consequently, the Mn $3d$ bandwidth should not be directly affected by the local stress induced by Ga^{3+} ions but solely by dilution. It has been found that some manganite systems undergo a structural transformation on cooling that affects their band structure.[29] In order to check this in our

system, we have collected x-ray patterns for $x=0.1$ down to 77 K. No structural changes have been detected except the typical thermal contraction. Therefore, any contribution from a structural transition can be discarded in $La_{2/3}Sr_{1/3}Mn_{1-x}Ga_xO_3$ for the range of Ga content studied.

B. Magnetic properties

The substitution of Ga for Mn leads to a weakening of the FM interactions in $La_{2/3}Sr_{1/3}Mn_{1-x}Ga_xO_3$ as evidenced by the decrease of both T_C and M_S and the subsequent loss of the FM long-range order at $x\sim0.3$ (this composition might be considered as a transitional one between ordered and non-ordered samples). The substitutional disorder, through a diminution of the number of Mn-Mn paths and an increase of the Mn^{4+}/Mn^{3+} ratio, promotes competitive magnetic interactions.[1] This, in turn, contributes to the magnetic frustration[30] that can give rise to the spin-glass-like behavior in the $x>0.3$ samples. We note that the doping range for which our system orders ferromagnetically ($0\leqslant x\leqslant 0.3$) is quite large in comparison to other doped manganites.[3-12] This may be attributed to the strong FM interactions between neighbor spins of the undoped compound $La_{2/3}Sr_{1/3}MnO_3$, as suggested by Alonso *et al.*[22]

C. Electrical transport properties

Disorder arising from doping tends to localize the current carriers and to decrease T_M. The increase of the activation energy with an increasing content of Ga (see Fig. 5) and the decrease of the resistive transition temperature in the system studied is consistent with these predictions. In addition, our studies show that, indeed, magnetic and resistive transitions do not occur at the same temperature for $x\geqslant0.05$. However, the magnetic transition is also clearly visible in the $\rho(T)$ curves, although a metalliclike state is achieved well below T_C.

The resistivity behavior in the system studied qualitatively follows the predictions of Ref. 22. It also agrees roughly with the results of a model for $La_{1-x}Sr_xMnO_3$-type compounds based on the double exchange mechanism and diagonal disorder.[20] However, a more direct comparision between these models and experimental data is difficult, since it involves too many arbitrary parameters. Our preliminary calculations show that the resistivity behavior for different values of x in $La_{2/3}Sr_{1/3}Mn_{1-x}Ga_xO_3$ can be explained as well in the framework of a random-resistor percolation-network model.[31] In this model, a sample (phase separated near T_C) is represented by an effective resistance corresponding to a parallel connection of resistances which represent the ferromagnetic conducting and paramagnetic insulating phases. At present, we cannot discriminate between these models.

Our experimental results can be summarized in the phase diagram shown in Fig. 9. We should point out that there is no true phase transition between FM metal and FM insulator regions. The dashed line in Fig. 9 merely divides regions with metalliclike and insulatinglike conductivities. Nevertheless, the magnetic ordering and the change of electrical behavior are uncoupled for $0.02<x<0.3$ samples.

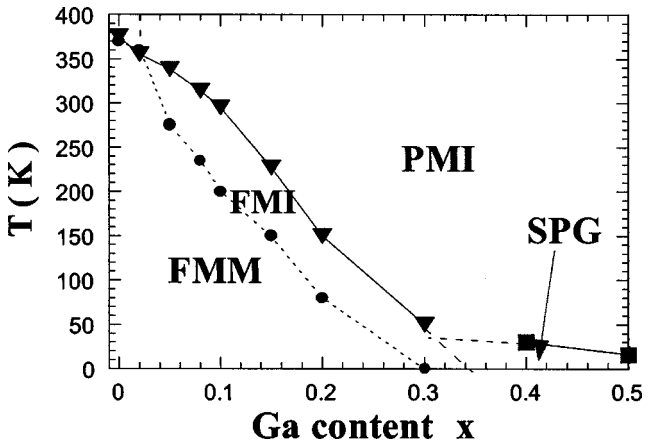

FIG. 9. Phase diagram for the $La_{2/3}Sr_{1/3}Mn_{1-x}Ga_xO_3$ series. PMI, FMI, FMM, and SPG refer to paramagnetic insulator, ferromagnetic insulator, ferromagnetic metal, and spin-(cluster-) glass phases, respectively.

The behavior of the magnetoresistance (MR) in the $La_{2/3}Sr_{1/3}Mn_{1-x}Ga_xO_3$ system is mainly determined by its granular nature. The low-field magnetoresistance (LFMR) in manganites is attributed to either spin-dependent scattering at the grain boundaries[32] or spin-dependent tunneling between grains.[27] Nonlinear current-voltage characteristics, obtained for a manganite bicrystal grain boundary, seem to point to the latter model.[33] An applied magnetic field, which aligns grains ferromagnetically, gives rise to larger electron tunneling and negative MR. Taking into account the magnetic field dependence of the intergrain coupling energy, one finds that $\Delta\rho/\rho_o\propto m^2/T$ in the ferromagnetic region, where m is the magnetization normalized to the saturation value.[27] The behavior of the MR found in our samples [Fig. 8(b)] is consistent with this prediction. LFMR also depends on the grain size.[28] Following the procedure used in Refs. 27 and 28, we have estimated the temperature variation of LFMR by finding the $H=0$ intercept of the extrapolated high-field MR and subtracting it from 1. We find that the LFMR increases with decreasing temperature, as expected. The temperature dependence of the LFMR for the $x=0.1$ sample, shown in the inset of Fig. 8, can reasonably be fitted by the function $a+b/(T+c)$. On the other hand, the field dependence of the HFMR is alike for temperatures below T_C. Its contribution to the total MR at 50 kOe is comparable to or even larger than that of the LFMR. It can be attributed to a tunneling process across a noncollinear surface layer at the grains.[34] However, more studies of $La_{2/3}Sr_{1/3}Mn_{1-x}Ga_xO_3$ samples with different grain sizes is needed to confirm this conclusion. In the paramagnetic region, carrier scattering by thermal spin disorder seems to be responsible for the observed $\rho(H)$ variation ($\Delta\rho/\rho_o\propto 1-m^2$).

Finally, we briefly discuss the low-temperature resistivity minimum observed in the system studied. This minimum shifts towards lower temperatures under an applied magnetic field and becomes shallower with increasing fields. The largest drop in $\rho(T,H)$ for this region occurs at $0\leqslant H\leqslant 5$ kOe. Tunneling between antiferromagnetically coupled grains can

once again be responsible for this behavior.[35] Such a model accounts fairly well for the resistivity minimum behavior in $La_{0.8}Sr_{0.2}MnO_3$.[36]

To summarize, our experimental results obtained for the $La_{2/3}Sr_{1/3}Mn_{1-x}Ga_xO_3$ system show that doping with Ga drastically affects the magnetic and electrical properties of this system in various ways. As both the Mn^{4+}/Mn^{3+} ratio and disorder increase with an increasing dilution of the magnetic sublattice, the Curie temperature sharply decreases and the system becomes more resistive. In particular, Ga doping leads to the uncoupling of the magnetic and resistive transitions in the system studied. Our results also show that the presence of grains and grain boundaries significantly modifies the electrical transport properties of this polycrystalline material in the presence of an external magnetic field.

ACKNOWLEDGMENTS

We thank J. L. Alonso and F. Guinea for fruitful discussions. This work was supported by CICyT (Spain) Project Nos. MAT02/01221 and MAT02/166.

*Corresponding author: I.C.M.A. Departamento de Física de la Materia Condensada C.S.I.C.-Universidad de Zaragoza Pedro Cerbuna, 12 50009 Zaragoza Spain. Fax: +34-976-761229. Email address: jbc@posta.unizar.es

[1] For a review, see J. M. D. Coey, M. Viret, and S. Von Molnar, Adv. Phys. **48**, 167 (1999); E. Dagotto, T. Hotta, and A. Moreo, Phys. Rep. **344**, 1 (2001).
[2] A. Urushibara, Y. Moritomo, T. Arima, A. Asamitsu, G. Kido, and Y. Tokura, Phys. Rev. B **51**, 14103 (1995).
[3] C. Zener, Phys. Rev. **82**, 403 (1951).
[4] M. R. Ibarra, P. A. Algarabel, C. Marquina, J. Blasco, and J. García, Phys. Rev. Lett. **75**, 3541 (1995).
[5] H. Y. Hwang, S. W. Cheong, P. G. Radaelli, M. Marezio, and B. Battlog, Phys. Rev. Lett. **75**, 914 (1995).
[6] J. Blasco, J. García, J. M. de Teresa, M. R. Ibarra, P. A. Algarabel, and C. Marquina, J. Phys.: Condens. Matter **8**, 7427 (1996).
[7] L. M. Rodríquez-Martínez and J. P. Attfield, Phys. Rev. B **54**, R15622 (1996).
[8] K. H. Ahn, X. W. Wu, K. Liu, and C. L. Chen, Phys. Rev. B **54**, 15299 (1996).
[9] X. Chen, Z. Wang, J. Cai, B. Shen, W. Zhan, and J. Chen, J. Appl. Phys. **86**, 4534 (1999).
[10] C. Osthöve, P. Grünberg, and R. R. Arons, J. Magn. Magn. Mater. **177–181**, 854 (1998); M. Sahana, K. Dörr, M. Doerr, D. Eckert, K.-H. Müller, K. Nenkov, L. Schultz, and M. S. Hedge, *ibid.* **213**, 253 (2000).
[11] Y. Sun, W. Tong, X. Xu, and Y. Zhang, Appl. Phys. Lett. **78**, 643 (2001); J. Gutierrez, A. Peña, J. M. Barandiarán, T. Hernández, L. Lezama, M. Insausti, and T. Rojo, Phys. Rev. B **56**, 1345 (1997).
[12] Q. Huang, Z. W. Li, J. Li, and C. K. Ong, J. Phys.: Condens. Matter **13**, 4033 (2001).
[13] J. Blasco, J. García, J. M. de Teresa, M. R. Ibarra, J. Pérez, P. A. Algarabel, C. Marquina, and C. Ritter, Phys. Rev. B **55**, 8905 (1997).
[14] M. C. Sánchez, J. Blasco, J. García, J. Stankiewicz, J. M. de Teresa, and M. R. Ibarra, J. Solid State Chem. **138**, 226 (1998).
[15] R. D. Shannon, Acta Crystallogr., Sect. A: Cryst. Phys., Diffr., Theor. Gen. Crystallogr. **32**, 751 (1976).
[16] S. M. Yusuf, M. Sahana, K. Dörr, U. K. Rößler, and K.-H. Müller, Phys. Rev. B **66**, 064414 (2002).
[17] Y. Sun, X. Xu, L. Zheng, and Y. Zhang, Phys. Rev. B **60**, 12 317 (1999).
[18] A. I. Coldea, S. J. Blundell, I. M. Marshall, C. A. Steer, J. Singleton, F. L. Pratt, L. D. Noailles, and M. J. Rosseinsky, L. E. Spring, and P. D. Battle, Phys. Rev. B **65**, 054402 (2001).
[19] P. D. Battle, S. J. Blundell, J. B. Claridge, A. I. Coldea, E. J. Cussen, L. D. Noailles, M. J. Rosseinsky, J. Singleton, and J. Sloan, Chem. Mater. **14**, 425 (2002).
[20] R. Allub and B. Alascio, Phys. Rev. B **55**, 14113 (1997).
[21] L. Sheng, D. Y. Xing, D. N. Sheng, and C. S. Ting, Phys. Rev. Lett. **79**, 1710 (1997).
[22] J. L. Alonso, L. A. Fernández, F. Guinea, V. Laliena, and V. Martín-Mayor, Phys. Rev. B **66**, 104430 (2002).
[23] J. L. Rodríguez-Carvajal, Physica B **55**, 191 (1992), J. L. Rodriguez-Carvajal and T. Roisnel, available at http://www-1lb.cea.fr/fullweb.
[24] M. Steins, W. Schmitz, R. Vecker, and J. Doerschel, Z. Kristallogr. - New Cryst. Struct. **212**, 76 (1997).
[25] A. M. Glazer, Acta Crystallogr., Sect. A: Cryst. Phys., Diffr., Theor. Gen. Crystallogr. **31**, 756 (1975).
[26] G. Subías, J. García, J. Blasco, and M. G. Proietti, Phys. Rev. B **57**, 748 (1998).
[27] H. Y. Hwang, S.-W. Cheong, N. P. Ong, and B. Batlogg, Phys. Rev. Lett. **77**, 2041 (1996).
[28] Ll. Balcells, J. Fontcuberta, B. Martínez, and X. Obradors, J. Phys.: Condens. Matter **10**, 1883 (1998).
[29] A. Asamitsu, Y. Moritomo, Y. Tomioka, T. Arima, and Y. Tokura, Nature (London) **373**, 407 (1995).
[30] J. A. Mydosh, *Spin glasses: An Experimental Introduction* (Taylor & Francis, London, 1993).
[31] M. Mayr, A. Moreo, J. Verges, J. Arispe, A. Feiguin, and E. Dagotto, Phys. Rev. Lett. **86**, 135 (2001).
[32] X. W. Li, A. Gupta, G. Xiao, and G. Q. Gong, Appl. Phys. Lett. **71**, 1124 (1997).
[33] R. Gunnarson, A. Kadigrobov, and Z. Ivanov, Phys. Rev. B **66**, 024404 (2002).
[34] Ll. Balcells, J. Fontcuberta, B. Martínez, and X. Obradors, Phys. Rev. B **58**, R14697 (1998).
[35] E. Rozenberg, M. Auslender, I. Felner, and G. Gorodetsky, J. Appl. Phys. **88**, 2578 (2000).
[36] M. Auslender, A. E. Kar'kin, E. Rozenberg, and G. Gorodetsky, J. Appl. Phys. **89**, 6639 (2001).